electronics

MDPI

Article

Battery Charging Procedure Proposal Including Regeneration of Short-Circuited and Deeply Discharged $LiFePO_4$ Traction Batteries

Pavol Spanik, Michal Frivaldsky *, Juraj Adamec and Matus Danko

Department of Mechatronics and Electronics, Faculty of Electrical Engineering and Information Technologies, University of Zilina, 010 26 Zilina, Slovakia; pavol.spanik@feit.uniza.sk (P.S.); juraj.adamec@feit.uniza.sk (J.A.); matus.danko@feit.uniza.sk (M.D.)

* Correspondence: michal.frivaldsky@fel.uniza.sk

Received: 20 April 2020; Accepted: 29 May 2020; Published: 2 June 2020

Abstract: The presented paper discusses the most often damages applying for lithium traction and non-traction cells. The focus is therefore given on investigation of possibilities related to the recovery of such damaged lithium-ion batteries, more specifically after long-term short-circuit and deep discharge. For this purpose, initially, the short-circuit was applied to the selected type of traction $LiFePO_4$ cell. Also, the deeply discharged cell was identified and observed. Both damaged cells would exhibit visible damage if electro-mechanical properties were measured. Individual types of damage require a different approach for battery regeneration to recover cells as much as possible. For this purpose, experimental set-up for automated system integrating proposed recovery methods were realized, while battery under test undergone a full-range of regeneration procedure. As a verification of the proposed regeneration algorithms, the test of delivered Ampere-hours (Ah) for various discharging currents was realized both for short-circuited as well as deeply discharged cells. Received results have been compared to the new/referenced cell, which undergoes the same test of delivered Ah. From the final evaluation is seen, that proposed procedure can recover damaged cell up to 80% of its full capacity if short-circuit was applied, or 70% if a deeply discharged cell is considered.

Keywords: traction battery; $LiFePO_4$; short-circuit; deep discharge; damage recovery

1. Introduction

Li-ion batteries have successfully penetrated our daily lives, from 3C products to EVs. For example, the newly developed Lithium Iron Phosphate ($LiFePO_4$) battery of larger energy capacity and safer chemical characteristics has been considered as an excellent power resource for future EVs. Anxiously, the capital costs of those Li-ion batteries are not low enough yet to substantially decrease the total EV cost for attracting numerous customers. Consequently, this fatal bottleneck directly impacts the universal adaptability of EVs. Some investigations delivered that the Li-ion battery cost needs to be chopped down around 50% for coming to EVs to compete against conventionally fueled vehicles with great odds [1–3] fully. Nowadays, in Europe, around 200 million vehicles are registered (approximately 80% are cars and 20% commercial vehicles). Car batteries deteriorate after two to three years, and people throw them away [4]. If only one battery from a total of five is replaced within a year, 15 million batteries are collected per year. Nevertheless, more than 15 million batteries are discarded only in Europe. Unfortunately, only one-third of the total quantity is recycled by manufacturers, and the rest is either eliminated or dumped in forests, rivers, and other places [5–7]. A significant reason for this increase in the number of used batteries is the short life cycle of lead-acid batteries. Besides, large-size batteries used for electric trucks are costly, with costs varying between 300 and 1500 euros, and hence

involve very high periodic expenses and then, more expensive products. Preventing the damage of this battery type and extending its life cycle will have a high economic impact [8–10].

Recycling, as well as regeneration/recovery of the used or harmed battery cells is, therefore, a topic, which must be accepted if sustainability related to environment and costs is considered [11–13]. Currently, the regeneration processes are available mostly for the lead-acid and NiMH batteries used for large electricity storage systems or hybrid vehicles. Target devices are batteries when both electrode plates are settled by crystallizes and electrolyte is composed solely of distilled water. A traditional battery charger will not be able to charge such a battery because it requires regeneration. The regeneration process consists commonly of a set of high-powered electrical pulses that are breaking down the crystallized layers. Battery regenerator manufacturers due to company know-how do not describe regeneration procedures, and each applies a separately developed system. Based on this, it is difficult to observe and determine the exact methodology used for regeneration [14–16].

Regarding the perspective of lithium-based cells used for e-mobility, the topic of regeneration will come to the forefront as the price of lithium is still high. Consequently, the manufacturing process of traction batteries represents an expensive procedure. Nowadays, many analyses, model development, and estimation algorithms for the state of charge and state of health have been developed, enabling to precisely estimate the operational life of traction energy storage systems [17–19]. However, there is a lack of studies dealing with the possibilities of regeneration of damaged cells, which after the correct capacity recovery process, could be used secondarily in the energy storage process.

Therefore, within the presented paper, the experimental methodology for damaged battery (focus is given on $LiFePO_4$ traction cells) considering various types of damage are introduced. Initially, the test with overcharging is provided, in order to verify protection components of investigated cells, and to verify the fact, whether regeneration on the overcharged battery can be applied. Consequently, the investigation of long-term short-circuit is presented together with the proposal and evaluation of the recovery algorithm suited for this type of battery damage. The proposed procedure is derived from the principles of regeneration of lead-acid batteries. In contrast, individual methods (regeneration from short-circuiting and regeneration from deep discharge) have been tested experimentally through variation of amplitudes of pulses, duration of pulses, and repetition (frequency) of pulses.

Similarly, the recovery procedure is proposed on the cells that take inappropriate long-term storage, where the deep discharge of the cell can apply. This situation is also described, while the recovery procedure with settings relevant for a deep discharge state was applied to damaged cells and consequently evaluated through the test of delivered ampere-hours. Received results have been compared to new cells and also evaluated after continual use (30 days of charging and discharging under various load) of regenerated pieces.

2. Electrical Types of Damage of Traction Batteries

Regarding the operation of batteries, there are several hazardous conditions related to the electrical behavior of the circuit, which can cause damage to the battery itself. Consequences coming from the wrong operation primarily reflect into the loss of the capacity or expressive, open-circuit voltage (OCV) drop. If the excessive duration of the hazardous operation is lasting, it can cause secondary harm to the internal structure as well as the mechanical cover of the battery. Here it is discussed long-term short-circuit operation, overcharging of the battery above permissible voltage level, or excessive deep discharge during battery operation or/and battery improper storage. Because each of the mentioned unwanted operational conditions reflects in battery damage, it is valuable to find whether the suitable procedure can be applied for battery regeneration back to its nominal operational state. In this article, the attention is focused on the investigation of the impact rate of improper operation, i.e., overcharging and short-circuit of 40 Ah–128 Wh Sinopoly $LiFePO_4$ 3.2 V battery. At the same time, a regeneration algorithm is applied on long term short-circuited cell. Similarly, deeply discharged cell WINA 60 Ah $LiFePO_4$ 3.2 V was observed and consequently subjected to the application of the proposed regeneration

procedure in order to restore its capacity and functionality. The main electrical parameters of both tested cells are listed in Table 1.

Table 1. Technical parameters of investigated cell Sinopoly $LiFePO_4$ 3.2 V 40 Ah.

Electrical Parameter	Sinopoly $LiFePO_4$ 3.2 V 40 Ah	WINA$LiFePO_4$ 3.2 V 60 Ah	
Nominal voltage	3.2	3.2	(V)
Maximum charging voltage	4	3.8	(V)
Minimum voltage	2.5	2.5	(V)
Maximum discharge current(continuous)	3	3	(C)
Optimal discharge current	13	20	(A)
Maximum charging current	80	90	(A)
Optimal charging current	13	20	(A)
Operating temperature	−45 to +85	−20 to +50	(°C)
Capacity	40	60	(Ah)
Shell material (package)	plastic	aluminum	(-)

2.1. Experimental Application of Overcharging

The experimental investigation of the first improper operational condition, i.e., overcharging of the battery, was realized with the use of test-stand, which is principally shown in Figure 1. The main device responsible for the simulation of the unwanted conditions is represented by programable power supply EA PSI 8080 (EA Elektro-Automatik GmbH & Co.KG, Viersen, Germany). It provides possibilities of programming of its output variables through instruction file, which covers information related to maximal values of charging voltage, current, and power as well for the predefined time interval. Recorded data of individual variables are stored in PC. For the analysis of visual damage observed over time, Canon EOS 6D is capturing images every 5 s, while thermal cameras FLIR E5 (FLIR, Boston, MA, USA). and FLIR SC660 (FLIR, Boston, MA, USA). are serving for detailed analysis of thermal performance during this experiment.

Figure 1. Block diagram of experimental test set-up for selected battery testing.

At the beginning of the test, the OCV of the battery was 3.43 V; thus, it refers to the charged state. According to the datasheet of the cell, the value of the charging voltage must not exceed 3.65 V. Initially, the selected overcharge value was set to 4.25 V, and the charging current was 10 A. CC&CV (Constant Current and Constant Voltage) charging mode was applied (Figure 2).

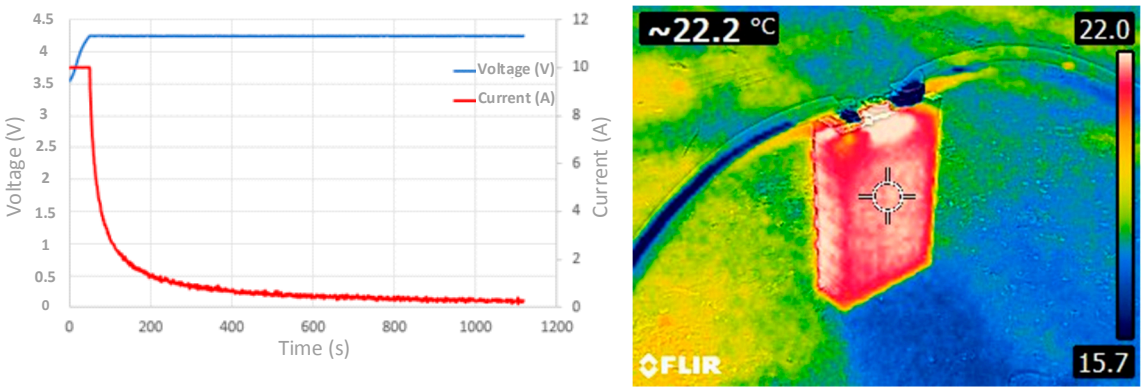

Figure 2. Waveforms of charging current and voltage during overcharging concerning for 4.25 V of charging voltage level.

The voltage on the battery reached the value of 4.25 V within the 50 s at a constant current of 10 A. From this point, the battery voltage was 4.25 V while the current was dropping gradually to almost 0 A. During the test, the temperature of the cell was maintained within the safe operating interval. At the same time, the maximum of 24.2 °C was achieved after 18 min and 36 s what represents 2.3 °C compared to the start of the test. During the experiment, no visible damage to the battery package was observed, and at the same time, no activation of the safety valve occurs. This test has continued with an increased level of charging voltage and current utilizing the same cell. Initially, for 35 s, 6.25 V/10 A was applied, while after 35 s, the level of charging current was increased to 30 A (Figure 3). After the 800 s of this test, the voltage on the cell reached 5.2 V. The package of the battery was corrupted, and the battery was irrefutably damaged because of the consequent electrolyte leak. This state was also reached due to the inactivation of the safety valve located between battery terminals. Based on these experiments, the limitations of the given types of traction cells have been verified. Exceeding allowable charging voltage above 5 V causes non-reversible damage to the battery. Thus, it is not possible to regenerate it or restore it. The only way is to recycle it for the second use.

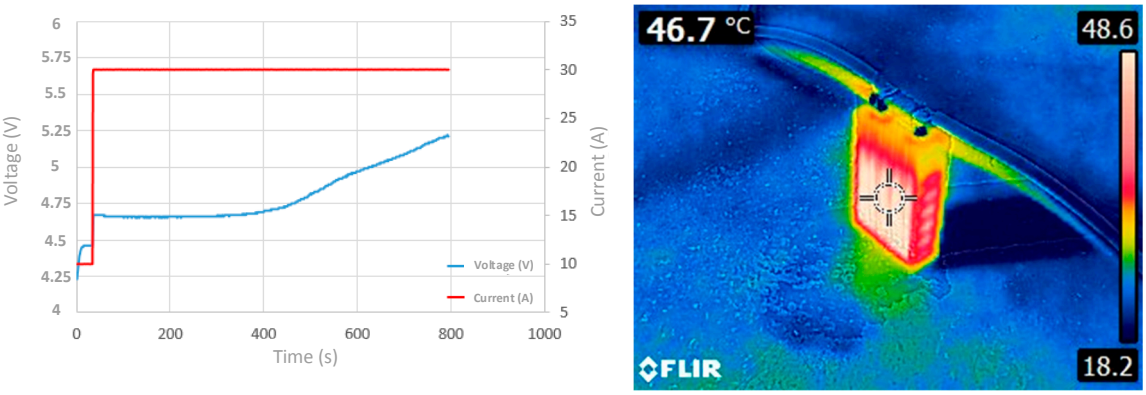

Figure 3. Waveforms of charging current and voltage during overcharging concerning 6.25 V of charging voltage level.

2.2. Experimental Application of Short-Circuit

The experiment of short-circuiting of selected $LiFePO_4$ 3.2 V, 40 Ah, 128 Wh battery cell was provided due to the requirement on the development of the recovery algorithm. Therefore, it was required to initially short-circuit selected cells for a given time interval in order to have a reference sample. From the safety point of view, short-circuit presents the most critical operational condition, because of the deformation of energy storage component that is caused by primarily—chemical and by secondarily—thermal issues. The experiment of the short-circuit was realized with the use of set-up

shown in Figure 4. This configuration uses thermo-vision camera FLIR E5 and thermo-vision camera FLIR SC 660.

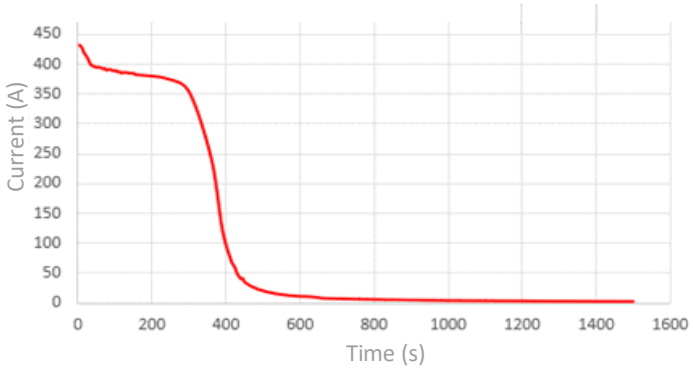

Figure 4. Time-waveform of short-circuit current during the experiment.

The utilization of both types is conditioned by the static and dynamic record of cell temperature. The measurement of short-circuit current was provided by APPA A18 (APPA Technology Corp., New Taipei City, Taiwan). Current meter, while values vs. time have been stored on PC through LabView measurement cards NI PXI 1031 (National Instruments, Austin, TX, USA). Camera Canon EOS 6D (Canon, Ota City, Tokio, Japan). was responsible for the acquirement of pictures in given time steps for the evaluation of cell's geometry shape changes.

Short-circuit was realized with the use of a new cell while it was initially formatted from the manufacturing process. Secondary formatting was done within laboratory conditions before the short-circuit experiment. The value of open-circuit voltage (OCV) before the test achieves 3.24 Vdc. For the start of the short-circuit test, the mechanical switch with a very high current rating was used.

Figure 4 shows the time-waveform of short-circuit current during the experiment. It is seen that after immediate shorting, the battery current reached over 430 A. Consequently, for more than 300 s, the battery was sourcing current over 350 A; its rapid drop is visible after 400 s of the short-circuit duration. The reduction to the value of 11.5 A and finally to 2.7 A was reached after more than 600 s. The total duration of this experiment was 25 min.

Together with the record of the value of short-circuit current, the thermal performance was also captured. At the end of the experiment, the surface temperature of the tested cell was 49.2 °C (Figure 5). The safety pressure valve located between the battery electrodes was not activated.

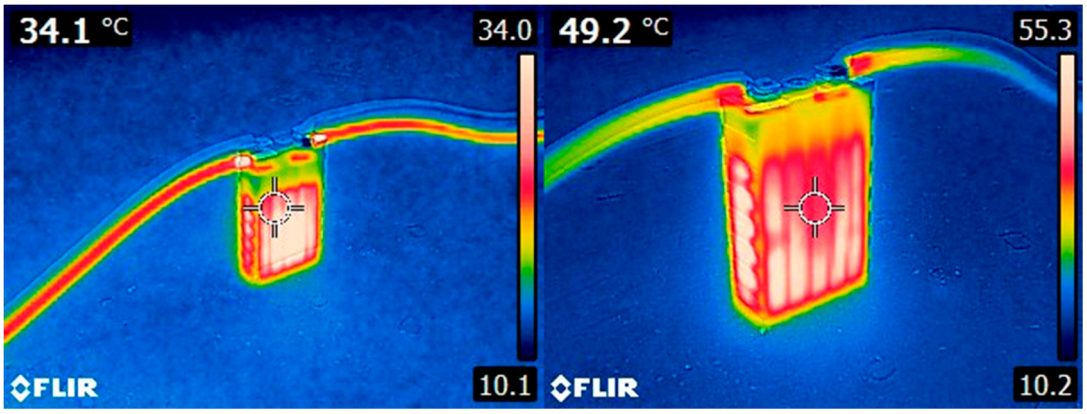

Figure 5. Maximal operational temperature of investigated battery during short-circuit operation.

Figure 6 indicates structural damages after completion of the short-circuit test. It is seen that the package of the cell is slightly flatulent. Geometrical measurements confirmed a visible increase of the

width dimension from 46 mm up to 54 mm. The maximum of 54 mm was measured in the middle of the height of the battery package.

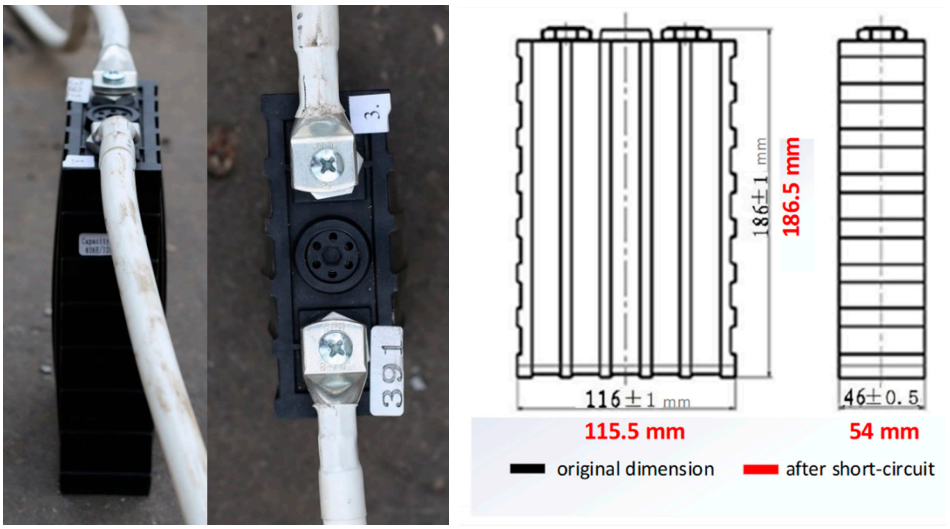

Figure 6. Geometrical changes of the cell package after short-circuit test.

After the experiment, the tested cell was left resting for 22 days. Dimensions of the package have been once checked after this period, while no change was observed compared to immediate evaluation after the short-circuit experiment.

2.3. Deep Discharge

Within the deep discharge testing, a 3.2 V 60 Ah $LiFePO_4$ cell was selected with significant damage to the cell's package. The measurement confirmed a deep discharge condition, while the open-circuit voltage of this cell was 1.88 V. The minimum voltage range for this cell is also 2.5 V, according to the datasheet (Table 1). An important fact is that the cell has a metal casing, which is primarily intended for increased protection against possible damage and heat dissipation. The tested cell represents an unused device, whereby deep discharge is a result of improper storage that has reached a critical level of voltage by self-discharge. It is determined by the manufacturer at a value of 3% of capacity over one month. Observation of the package of this cell discovers visible inflation within the central part, while the width reached 43.8 mm (Figure 7). The original cell's width stated by the manufacturer is 36 mm.

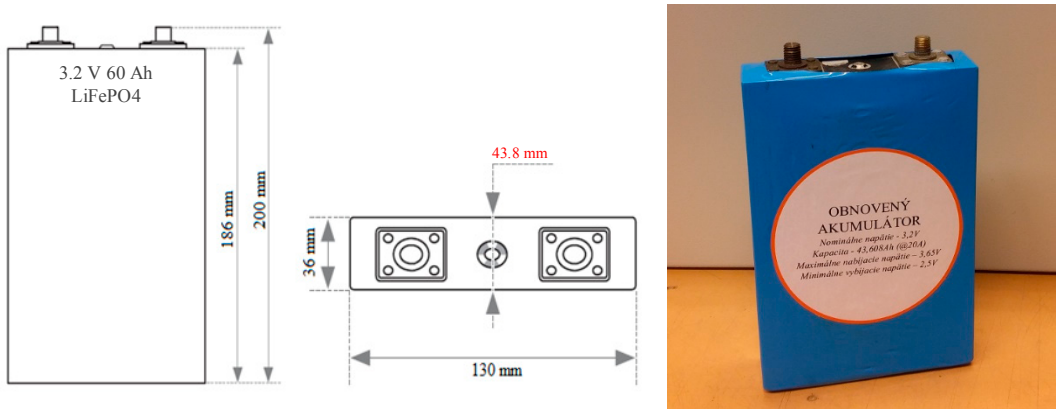

Figure 7. Evaluation of geometrical changes valid for center points of the width of deeply discharged cell (**left**) and a physical sample of this cell (**right**).

3. Regeneration Procedure Proposal for Short-Circuited and Deep Discharged Cells

The device under test is located within a metal box, while required measurements are realized with the use of laboratory equipment given on Figure 8. The mechanical switch protects the power line from the source/load to the battery preventing a hazardous situation. The programable electronic load KIKOSUI PLZ 100 W and programable DC source EA PSI 8080-60 are controlled by LabView interface, which also provides data logging of the measured values (cell's—current/voltage/temperature). Through a developed user guide, it is possible to program various scenarios related to recovery algorithms, i.e., charging sequences and discharging sequences.

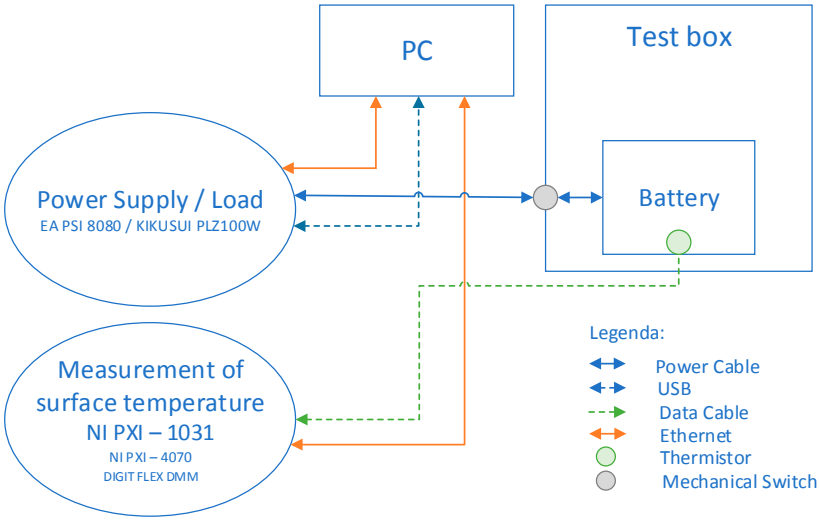

Figure 8. Block diagram of test-stand for traction batteries recovery.

3.1. Proposal for Regeneration Algorithm of Short-Circuited Cell

The proposed recovery process is suited for 3.2 V, 40 Ah, $LiFePO_4$, while its use is available for various Li-Fe phosphate cells. The only change lies in the consequent modification of individual charging steps, considering maximum allowable charging current and voltage. After the proposed recovery method is applied, its effect will be evaluated by the test of obtained Ah of the recovered cell.

The initial check of the harmed cell was focused on the evaluation of OCV, whose value was 2.83 V. This refers to the fully discharged state, while the value of OCV after long-term short circuit is still between the limits of operational values of the cell defined by the datasheet. For the selected type, the limits are within 2.5 V ± 3.65 V.

The battery recovery aims to reduce the negative impacts of the short-circuit consequences on the electrical and mechanical properties of DUT (device under test).

The proposal is based on the charging sequences, which are characterized by the pulsed current (Figure 9). These charging sequences are split into six groups. After each of the sequences, the resting period is applied (app. 16 h). The duration of each pulse sequence was lasting 100 min, whereby four cycles (25 min each) developed one sequence. The main difference between the cycles is the amplitude of charging current (Table 2).

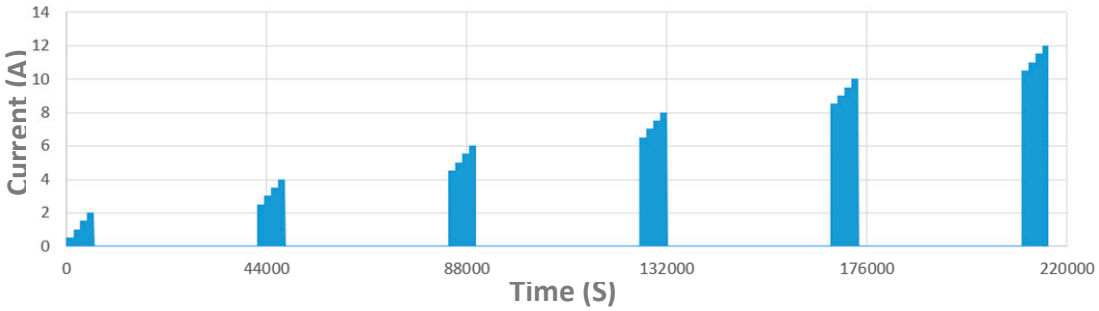

Figure 9. Graphical interpretation of proposed regeneration procedure for short-circuited cells including resting periods of DUT.

Table 2. The setting of individual sequences of regeneration algorithm for short-circuited cell.

Sequence	Duration	The Amplitude of Charging Current	Charging Voltage
1	100 min 4 cycles × 25 min	0.5 A–2 A each cycle 0.5 A increase	3.65 V
2	100 min 4 cycles × 25 min	2.5 A–4 A each cycle 0.5 A increase	3.65 V
3	100 min 4 cycles × 25 min	4.5 A–6 A each cycle 0.5 A increase	3.65 V
4	100 min 4 cycles × 25 min	6.5 A–8 A each cycle 0.5 A increase	3.65 V
5	100 min 4 cycles × 25 min	8.5 A–10 A each cycle 0.5 A increase	3.65 V
6	100 min 4 cycles × 25 min	10.5 A–12 A each cycle 0.5 A increase	3.65 V

Figure 10 shows the time waveform of the battery voltage and temperature during the first charging sequence. It is seen that the initial OCV value was 2.83 V, while at the end of the charging sequence, the value reached 2.97 V.

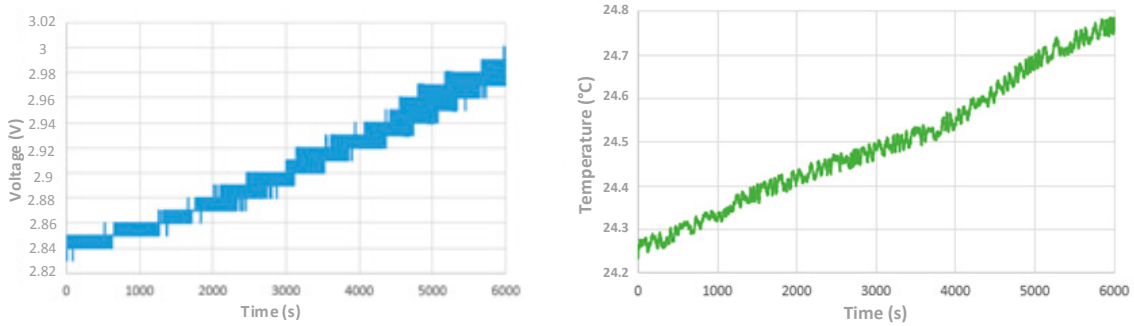

Figure 10. Time waveform of battery voltage (**left**) and its surface temperature (**right**) during the first regeneration sequence.

After the last 16 h of regeneration, the last sequence was applied, while OCV drops to 3.26 V what is a difference of 0.11 V compared to the end of the fifth charging sequence (Figure 11). The current range within the sixth cycle is 10.5 A up to 12 A. The value of the battery voltage at the end was 3.42 V, while after final 16 h of resting period OCV reached 3.31 V. The temperature profile during each regeneration sequence has shape similar to characteristics shown on Figures 10 and 11 as well.

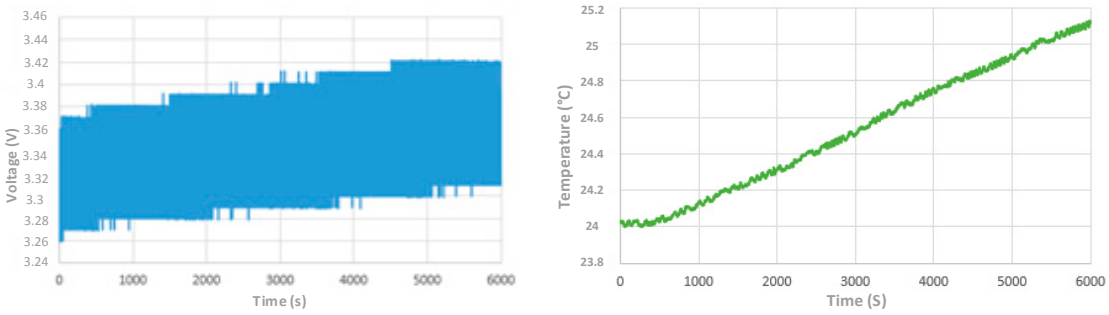

Figure 11. Time waveform of battery voltage (**left**) and its surface temperature (**right**) during last regeneration sequence.

DUT has completed six charging sequences. After 18 h of regeneration from the last sixth charging sequence, the open-circuit voltage reached 3.27 V. From the viewpoint of the safety of cell operation during the application of the charging sequences, no significant increase in the surface temperature or change in the dimensions of the external structure was observed.

The main reason for the cycling of each subsequence was to ensure a gradual increase in the charging current. The pause interval between charging steps is essential for battery recovery. In terms of reliability, the battery is currently stable and ready for a full charge. The level of its usability will be evaluated based on the test of delivered ampere-hours.

3.2. Proposal for Regeneration Algorithm of Deeply Discharged Cell

As discussed earlier, the 3.2 V 60 Ah, $LiFePO_4$ cell was selected for the application of a regeneration algorithm while deep discharge (1.88 V) of the DUT is considered. Compared to the regeneration of the short-circuited cell, this algorithm is divided into 30 charging cycles and 30 cycles of pause mutually alternating, whereby one cycle is lasting 1 s (Table 3). After it, 5 min of regeneration is applied to DUT (Figure 12). One sequence of regeneration algorithm valid for deep discharge was lasting 126 min. The charging current impulse had an amplitude of 20 A, which refers to 1/3 of the capacity of the cell. The amplitude of the charging voltage was 3.65 V. For the given battery, the application of six sequences was realized in order to achieve the required OCV on the device. At the same time, 16 h of the resting period was applied between individual sequences.

Table 3. The setting of sequences of regeneration algorithm for deeply discharged cell.

	Duration	**The Amplitude of Charging Current**	**Charging Voltage**
Sequence	126 min consists of subsequences 1 and 2	20 A	3.65 V
Subsequence 1	30 charging pulses 30 pause pulses alternating one pulse = 1 s		
Subsequence 2	Regeneration period 5 min		

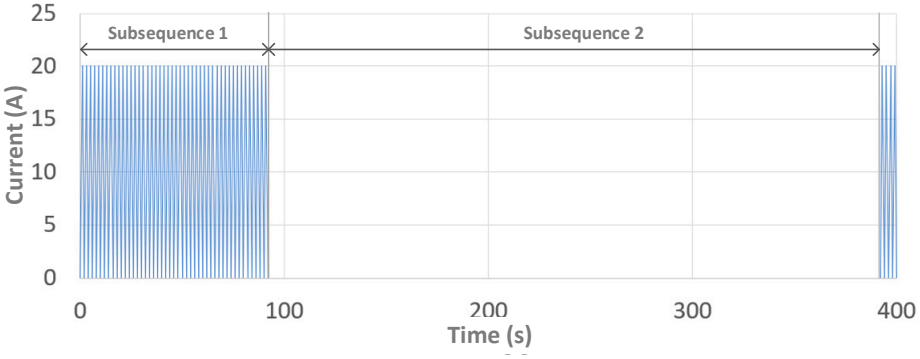

Figure 12. Graphical interpretation of the proposed regeneration sequence for deeply discharged cells.

Figure 13 shows the time waveform of battery voltage during the application of the first regeneration sequence and last (six) regeneration sequence (Table 4). It is seen that voltage raised from 2.04 V up to 3.19 V at the end of the first sequence. During the last sequence, the voltage level on the cell exceeds 3.3 V. The temperature on the cell during each sequence was within 25.38 °C–26.18 °C.

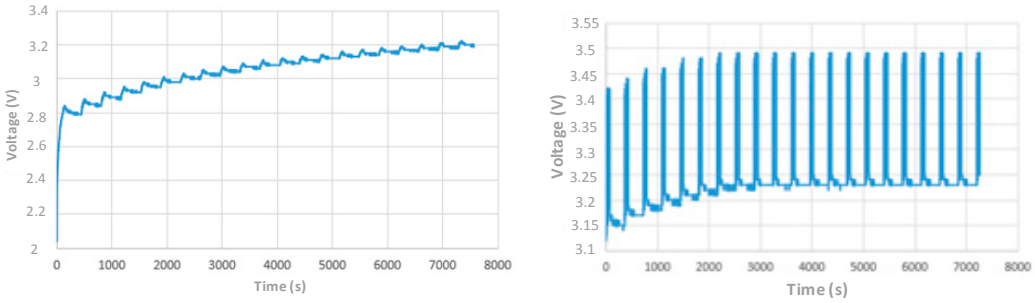

Figure 13. The voltage waveform of initially deeply discharged cell after application of the first sequence of regeneration algorithm (**left**) and the last, sixth sequence (**right**).

Table 4. Voltage levels before and after each regeneration sequence of deeply discharged cell.

Sequence	The Voltage on the Cell before the Sequence	The Voltage on the Cell after the Sequence
1	2.04 V	3.19 V
2	3.12 V	3.21 V
3	3.19 V	3.27 V
4	3.21 V	3.28 V
5	3.24 V	3.29 V
6	3.26 V	3.31 V

4. Verification of Recovered Cells Through the Test of Delivered Ampere-Hours

At the beginning of this test, it is required to charge recovered batteries fully. For selected types of batteries, CC&CV charging (Constant Current and Constant Voltage) is recommended. Both recovered batteries are verified in the way of delivered ampere-hours test (test of capacity), whereby new un-damaged cells have been used as reference devices for comparisons and evaluation.

For the test of battery capacity, five discharging scenarios have been verified. Each scenario is characterized by a different value of discharging current, while the range was selected based on the operational properties of selected cells (13 A/20 A–120 A). After each test, the cell was re-charged to full capacity.

4.1. Verification of Regeneration Algorithm of Short-Circuited Cell

Test of the capacity of the short-circuited cell was realized for five values of discharging currents, i.e., 13 A, 20 A, 40 A, 80 A, and 120 A. Initially recovered cell was tested. At the same time, consequently, the reference sample has undergone a similar test. The profiles of battery voltage during individual discharging states for the recovered and new cell are graphically interpreted on Figures 14–16.

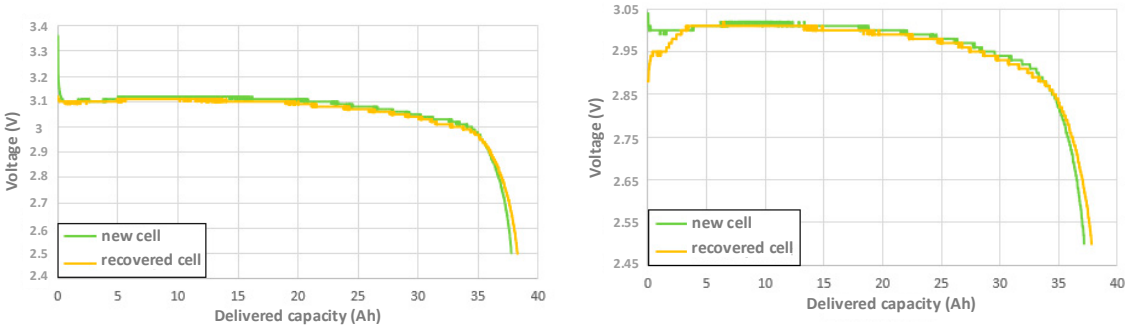

Figure 14. Voltage profile during discharge by 13 A (**left**) and 20 A (**right**) for regenerated (yellow) and referenced cell (green).

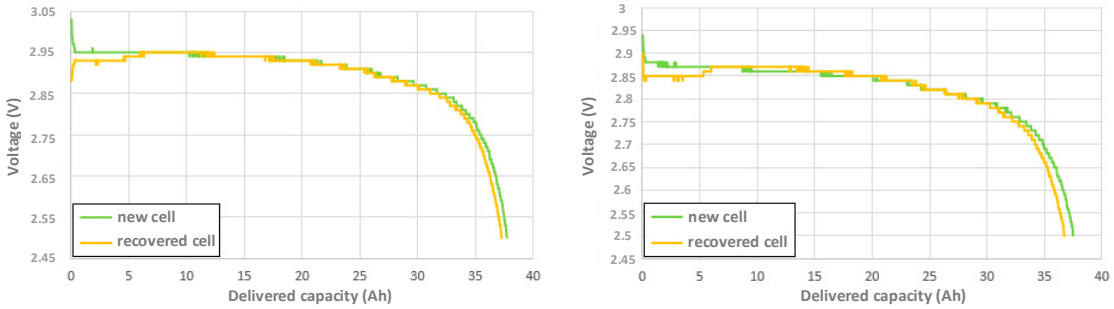

Figure 15. Voltage profile during discharge by 40 A (**left**) and 80 A (**right**) for regenerated (yellow) and referenced cell (green).

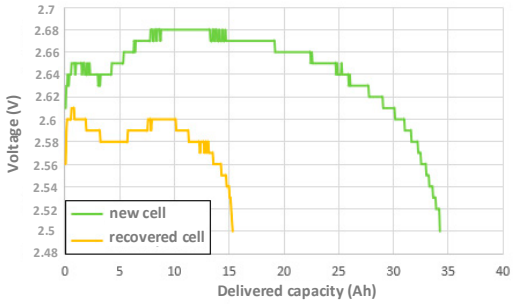

Figure 16. Voltage profile during discharge by 120 A for regenerated (yellow) and referenced cell (green).

From Figures 14 and 15 is visible that for discharging current between 13 A–80 A recovered cell is delivering a similar number of ampere-hours compared to the new cell. The visible difference is valid for the case of 120 A (Figure 16), where the recovered cell provides just half of the capacity of the new cell. A detailed summary of the results from this test is listed in Table 5.

Table 5. Summary of the results of the verification test of short-circuited cell.

Battery Cell Model	**3.2 V, 40 Ah, $LiFePO_4$**	**3.2 V, 40 Ah, $LiFePO_4$**
Cell Status	**Recovered after Short-Circuiting**	**New Cell**
	Discharge CC 20 A	
Discharge time	1 h, 52 min, 54 s	1 h, 51 min
Ambient temperature	20.105 °C	21.451 °C
Maximal surface temperature	28.1 °C	30.253 °C
Delivered Ah	38.297 Ah	37.752 Ah
	Discharge CC 40 A	
Discharge time	55 min, 44 s	54 min, 26 s
Ambient temperature	20.677 °C	21.054 °C
Maximal surface temperature	29.684 °C	31.374 °C
Delivered Ah	37.812 Ah	37.163 Ah
	Discharge CC 60 A	
Discharge time	36 min, 48 s	36 min, 52 s
Ambient temperature	21.264 °C	21.984 °C
Maximal surface temperature	32.86 °C	33.036 °C
Delivered Ah	37.303 Ah	37.726 Ah
	Discharge CC 80 A	
Discharge time	27 min, 41 s	27 min, 34 s
Ambient temperature	20.384 °C	21.453 °C
Maximal surface temperature	34.788 °C	34.346 °C
Delivered Ah	36.755 Ah	37.482 Ah
	Discharge CC 120A	
Discharge time	7 min, 47 s	16 min, 44 s
Ambient temperature	21.116 °C	20.998 °C
Maximal surface temperature	28.186 °C	35.027 °C
Delivered Ah	15.313 Ah	34.236 Ah

4.2. Verification of Regeneration Algorithm of Deeply Discharged Cell

The second verification test of the recovery algorithm for the deeply discharged cell was realized for four values of discharging currents, i.e., 20 A, 40 A, 60 A, and 80 A. Recovered cell was compared with unused (new) cell, which was initially formatted.

Figure 17 shows the voltage profile of recovered and new cells for 20 A and 40 A of discharging current. For 20 A situation, the new cell delivers an app. 60 Ah, more precisely 60.869 Ah during 3 h 2 min 46 s. The highest temperature on the surface of the cell achieved 35.397 °C. On the other side, the recovered cell delivers just 43.608 Ah what is more than 17 Ah less compared to the new cell. For the test with 40 A of discharging current, the new cell delivered 59.468 Ah and recovered 42,536 Ah. During both tests, the temperature on the surface of the cell raised to 39.16 °C, i.e., 3.46 °C more compared to the recovered cell.

Voltage profiles for the tests with 60 A and 80 A are shown on Figure 18. It is seen that for both situations, the new cell can deliver approximately 56 Ah (surface temperature 44.168 °C). In contrast, recovered cell behaves similar to previous tests, if 60 A discharge is considered (app. 40 Ah is delivered). However, if 80 A of discharge is applied to the recovered cell, its voltage drops to the minimum cell voltage. Thus, this situation almost represents the hazardous case. The amount of delivered Ah reached 35.886 Ah (surface temperature 40.881 °C). The summary of all tests is listed in Table 6.

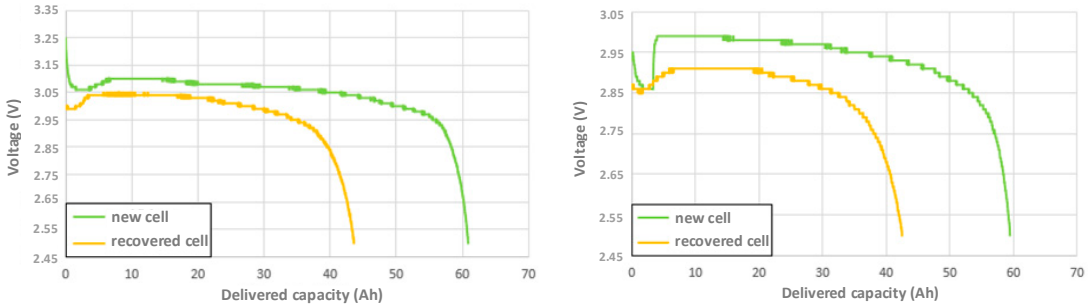

Figure 17. Voltage profile during discharge by 20 A (**left**) and 40 A (**right**) for regenerated (yellow) and referenced cell (green).

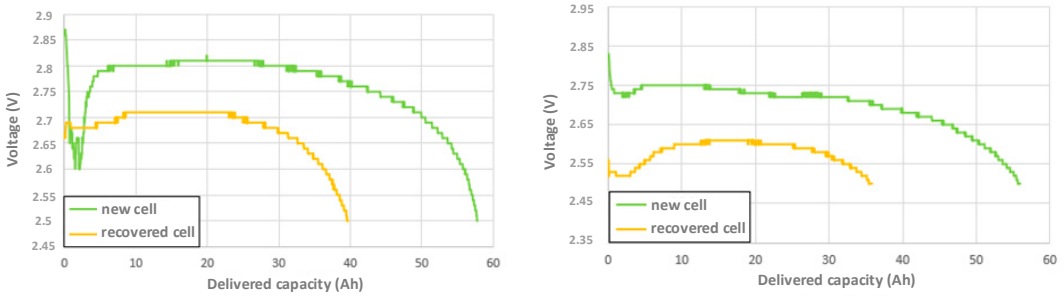

Figure 18. Voltage profile during discharge by 60 A (**left**) and 80 A (**right**) for regenerated (yellow) and referenced cell (green).

Table 6. Summary of the results of the verification test of deeply discharged cell.

Battery Cell Model	**3.2 V, 60 Ah, $LiFePO_4$**	**3.2 V, 60 Ah, $LiFePO_4$**
Cell Status	**Recovered after Deep Discharge**	**New Cell**
	Discharge CC 20 A	
Discharge time	2 h, 8 min, 18 s	3 h, 2 min, 46 s
Ambient temperature	21.238 °C	22.018 °C
Maximal surface temperature	31.293 °C	35.397 °C
Delivered Ah	43.608 Ah	60.869 Ah
	Discharge CC 40 A	
Discharge time	1 h, 2 min, 40 s	1 h, 27 min, 18 s
Ambient temperature	21.896 °C	21.997 °C
Maximal surface temperature	35.703 °C	39.158 °C
Delivered Ah	42.536 Ah	59.486 Ah
	Discharge CC 60 A	
Discharge time	38 min, 58 s	57 min, 47 s
Ambient temperature	20.891 °C	22.321 °C
Maximal surface temperature	38.403 °C	41.502 °C
Delivered Ah	39.709 Ah	57.826 Ah
	Discharge CC 80 A	
Discharge time	26 min, 22 s	41 min, 4 s
Ambient temperature	21.574 °C	22.054 °C
Maximal surface temperature	40.881 °C	44.168 °C
Delivered Ah	35.886 Ah	55.965 Ah

5. Conclusions

In this paper, the experimental investigation of the recovery algorithms of the traction batteries with lithium phosphate technology has been studied with selected types of cells. The main focus was

given on possibilities related to the renewal of initially damaged cells by long-term short-circuit or deep discharge. For both situations, procedures are based on the charging process. Thus, individual procedures propose a different approach, i.e., the short-circuited cell requires gradual medium duration profile of charging sequences (with an increase of charging current), whereby deeply discharged cell uses short duration peak charging pulses. Both proposals have been experimentally verified in the way of the test of delivered ampere-hours of restored cells. The comparisons of these tests have been made with newly formatted cells of the same type. From experiments was found that short-circuited battery is capable of recovering up to 80% if the proposed recovery procedure is applied. It is valid for discharge currents within 20 A–80 A (0.5 °C–2 °C). For higher currents, the recovery represents an app. 55%. From these results can be said, that recovered cell after long-term short-circuit is capable of second use. At the same time, restrictions must be respected related to the value of continuous discharging current. A similar result was achieved if the deeply discharged cell was verified. The recovery achieved almost 70% if discharge currents are within 0.3 °C–0.6 °C. For higher currents, the voltage drop of the battery represents limiting parameters as it reaches the minimum allowable operational value.

Batteries were tested with an ampere-hour test after the initial testing sequence ten times in a row after 28 days of storage. Differences in capacity values between repeated tests were lower than 2%. From received results, the expectations for long-term regenerated battery use is possible regarding recovered capacity, which is lower than nominal capacity. Restrictions on discharging currents must also be accepted, i.e., it is not recommended to use high operating currents. Consequently, it is proposed to use accelerated pulsed charging instead of the CV/CC method to slow down degradation lengthening operational life.

It must be said here that the same results have been achieved after 28 days of these tests. The proposed methodology gives proper way, how to recover damaged lithium cells.

Author Contributions: Conceptualization, P.S., methodology, J.A., experimental analysis and set-ups, M.D.; writing—original draft preparation, M.F. All authors have read and agreed to the published version of the manuscript.

Funding: This research was funded by APVV-15-0396 and APVV-15-0571. The experimental support was also done by project funding Vega 1/0547/18.

Acknowledgments: The authors would like to thank to Slovak national grant agencies APVV and Vega for the above mentioned financial support.

Conflicts of Interest: The authors declare no conflicts of interest.

References

1. Propfe, B.; Redelbach, M.; Santini, D.J.; Friedric, H. Cost Analysis of Plug-In Hybrid Electric Vehicles Including Maintenance & Repair Costs and Resale Values (Conference EVS26). 2012. Available online: https://www.mdpi.com/2032-6653/5/4/886 (accessed on 25 May 2020).
2. Nykvist, B.; Nilsson, M. Rapidly falling costs of battery packs for electric vehicles. *Nat. Clim. Chang.* **2015**, *5*, 329. [CrossRef]
3. Scrosati, B. History of lithium batteries. *J. Solid State Electrochem.* **2011**, *15*, 1623–1630. [CrossRef]
4. Brodd, R. *Batteries for Sustainability: Selected Entries from the Encyclopedia of Sustainability Science and Technology*; Springer: New York, NY, USA, 2013; Volume VI, p. 513. ISBN 978-1-4614-5791-6.
5. Aditya, P.J.; Ferowsi, M. Comparison of NiMh and Li-ion batteries in automotive applications. In Proceedings of the Vehicle Power and Propulson Conference, Harbin, China, 3–5 September 2008.
6. Yoo, H.D.; Markevich, E.; Salta, G.; Sharon, D.; Aurbach, D. On the challenge of developing advanced technologies for electrochemical energy storage and conversion. *Mater. Today* **2014**, *17*, 110–121. [CrossRef]
7. Tarascon, J.M.; Armand, M. Issues and challenges facing rechargeable lithium batteries. *Nature* **2001**, *414*, 359–367. [CrossRef] [PubMed]
8. Becker, J.; Schaeper, C. Design of a safe and reliable li-ion battery system for applications in airbone system. In Proceedings of the 52nd AIAA Aerospace Sciences Meeting-AIAA Science and Technology Forum and Exposition, National Harbor, MD, USA, 13–17 January 2014; SciTech: Wellesley Park, NC, USA, 2014.

9. Chamnan-arsa, S.; Uthaichana, K.; Kaewkham-ai, B. Modeling of $LiFePO_4$ battery state of charge with recovery effect as a three-mode switched system. In Proceedings of the 2014 13th International Conference on Control, Automation Robotics & Vision (ICARCV), Singapore, 10–12 December 2014; pp. 1712–1717. [CrossRef]
10. Cai, Y.; Zhang, Z.; Zhang, Y.; Liu, Y. A self-reconfiguration control regarding recovery effect to improve the discharge efficiency in the distributed battery energy storage system. In Proceedings of the 2015 IEEE Applied Power Electronics Conference and Exposition (APEC), Charlotte, NC, USA, 15–19 March 2015; pp. 1774–1778. [CrossRef]
11. Huang-Jen, C.; Li-Wei, L.; Ping-Lung, P.; Ming-Hsiang, T. A novel rapid charger for lead-acid batteries with energy recovery. *IEEE Trans. Power Electron.* **2006**, *21*, 640–647. [CrossRef]
12. Stefan-Cristian, M.; Cornelia, C.A.; Stefan, U. Battery regeneration technology using dielectric method. In Proceedings of the 2014 International Conference and Exposition on Electrical and Power Engineering (EPE), Iasi, Romania, 16–18 October 2014; pp. 839–844. [CrossRef]
13. Orchard, M.E.; Lacalle, M.S.; Olivares, B.E.; Silva, J.F.; Palma-Behnke, R.; Estévez, P.A.; Cortés-Carmona, M. Information-Theoretic Measures and Sequential Monte Carlo Methods for Detection of Regeneration Phenomena in the Degradation of Lithium-Ion Battery Cells. *IEEE Trans. Reliab.* **2015**, *64*, 701–709. [CrossRef]
14. Amanor-Boadu, J.M.; Guiseppi-Elie, A. Improved Performance of Li-ion Polymer Batteries Through Improved Pulse Charging Algorithm. *Appl. Sci.* **2020**, *10*, 895. [CrossRef]
15. Kirpichnikova, I.; Korobatov, D.; Martyanov, A.; Sirotkin, E. Diagnosis and restoration of li-Ion batteries. *J. Phys. Conf. Ser.* **2017**. [CrossRef]
16. Medora, K.N.; Kusko, A. An Enhanced Dynamic Battery Model of Lead-Acid Batteries Using Manufacturers Data. In Proceedings of the INTELEC 06—Twenty-Eighth International Telecommunications Energy Conference, Providence, RI, USA, 10–14 September 2006; pp. 1–8. [CrossRef]
17. Cacciato, M.; Nobile, G.; Scarcella, G.; Scelba, G. Real-Time Model-Based Estimation of SOC and SOH for Energy Storage Systems. *IEEE Trans. Power Electron.* **2017**, *32*, 794–803. [CrossRef]
18. Liu, J.; Chen, Z. Remaining Useful Life Prediction of Lithium-Ion Batteries Based on Health Indicator and Gaussian Process Regression Model. *IEEE Access* **2019**, *7*, 39474–39484. [CrossRef]
19. Baghdadi, I.; Briat, O.; Deletage, J.Y.; Vinassa, J.M.; Gyan, P. Dynamic Battery Aging Model: Representation of Reversible Capacity Losses Using First Order Model Approach. In Proceedings of the 2015 IEEE Vehicle Power and Propulsion Conference (VPPC), Montreal, QC, USA, 19–22 October 2015; pp. 1–4. [CrossRef]

© 2020 by the authors. Licensee MDPI, Basel, Switzerland. This article is an open access article distributed under the terms and conditions of the Creative Commons Attribution (CC BY) license (http://creativecommons.org/licenses/by/4.0/).